Liquid laminated glass connections

Stratis Volakos[1], Chris Davis[2], Martien Teich[3], Peter Lenk[4], Mauro Overend[5]

1 University of Cambridge, Cambridge (United Kingdom), ev338@cam.ac.uk

2 H. B. Fuller | Kömmerling, Pirmasens (Germany), Chris.Davis@koe-chemie.de

3 seele, Gersthofen (Germany), martien.teich@seele.com

4 Arup, London (United Kingdom), Peter.Lenk@arup.com

5 Delft University of Technology (TU Delft), Delft (Netherlands), M.Overend@tudelft.nl

Connections between structural glass components play a major role in terms of the structural integrity and aesthetics of glass applications. Recently, a promising type of adhesive connection, known as embedded laminated glass connections, has been developed. The main shortcomings of this connection are the high fabrication costs and that residual stresses arise during the autoclave lamination process that result in reduced connection strength. In this study, a variant of this connection is examined where lamination is achieved by means of a cold-poured resin to reduce fabrication costs and eliminate unfavourable residual stresses. Specifically, this paper presents the results of the fabrication methodology and the structural performance assessment of physical prototypes of the proposed connection. The latter is investigated via Finite Element Analysis (FEA) conducted on the connection 3D numerical model which is validated by experimental pull-out tests performed on the physical prototypes. Overall, it is found that the prototypes are satisfactory in terms of manufacturability and aesthetics and they also achieve considerable load-bearing capacity with notable ductility at failure.

Keywords: Embedded glass connection, Fabrication methodology, Pull-out tests, Numerical model

1 Introduction

Loadbearing connections between structural glass components are very challenging because they need to transmit high forces in a material that is sensitive to stress concentrations and they must do so in a visually unobtrusive manner. To date, bolted joints constitute the most common method for connecting glass components. However, the work of Overend et al. [1] showed that the load-bearing capacity of adhesive joints exceeds that of their bolted counterparts. Recently, a novel adhesive connection has emerged that has made step-change improvements in the load-bearing capacity and the aesthetics of structural glass connections. This connection is known as embedded laminated glass connections and it has been implemented successfully in real-world projects (O'Callaghan [2], Torres et al. [3]).

Embedded laminated connections consist of laminated glass where a metallic insert is embedded by means of a polyvinyl butyral (PVB) or an ionoplast (SG) transparent solid foil interlayer (Belis et al. [4], Puller and Sobek [5], Carvalho et al. [6], Marinitsch et al. [7], Santarsiero et al. [8], [9], Bedon and Santarsiero [10], Louter and Santarsiero [11]). To date, such connections are typically manufactured via the standard autoclave lamination process where the glass, the metallic insert and the adhesive material are placed in a vacuum bag and subjected to temperature-pressure (up to 140 °C and 14 bar) cycles. As a consequence, undesirable residual stresses emerge in the vicinity of the connection due to the autoclaving process, particularly due to the heating/cooling of materials with different coefficients of thermal expansion (glass and metallic insert). To mitigate these stresses, titanium (Torres et al. [3]) is often used because its coefficient of thermal expansion is similar to glass. However, the combined cost of titanium and the autoclaving process makes these connections relatively expensive.

This study constitutes a variant of the embedded connections, where a steel insert is embedded within the laminated glass component by means of a transparent cold-poured resin. The first part of this study presented in this paper, provides a detailed description of the liquid lamination process along with the numerical (FEA) and experimental results of destructive tensile pull-out tests conducted on physical prototypes of the connection at room temperature. This study will form the basis of further pull-out tests to be performed at different temperatures and strain rates to account for the influence of the viscoelastic behaviour of the resin interlayer on the connection performance.

2 Specimens

The pull-out specimens (Fig. 2-1) consist of a laminated glass unit comprising of two heat-strengthened glass plies (EN 1863-1:2000) where a steel insert is embedded along one long edge (embedment glass edge). In order to achieve high transparency and thus enhanced aesthetics, low iron (high-clarity) glass with polished edges has been selected. The dimensions of the two glass plies are 300 x 400 x 6 mm. The 100 x 200 x 2 mm insert is made of 1.4404 (EN 10088-3:2005) stainless steel. The insert has an embedded length of 100 mm and rounded edges *(R*=5 mm*)* at its end face to minimise stress concentrations. To ensure good adhesion, the steel insert is polished to a surface roughness (Ra) of 0.2 mm. Lamination is achieved by means of a transparent two-component polyurethane-based liquid composite resin (Ködistruct LG [12]) whose pot life can be adjusted from 10 to 60 minutes. The resin chemical curing (exothermic reaction) is mostly completed within seven days at room temperature but it can be moved and handled much earlier (within approximately 48 hours). The thickness of the resin interlayer between the steel insert and the glass plies is 2 mm while its total thickness (away from the embedded area) is 6 mm.

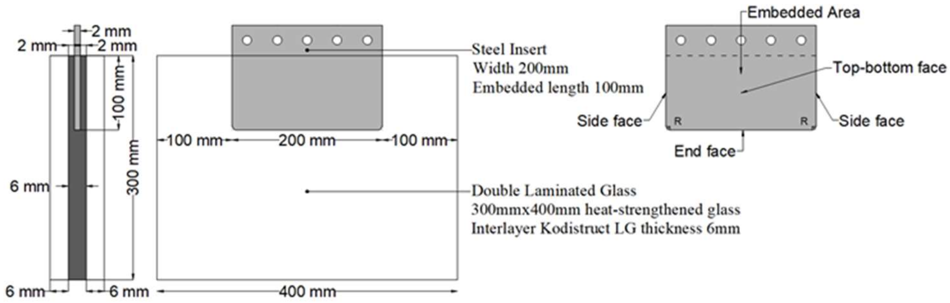

Figure 2-1 Pull-out specimen; section (left) and top view (right).

3 Fabrication Methodology

All specimens were laminated by the author and support staff at the H. B Fuller | Kömmerling Liquid Composite Centre of Excellence at TTec GmbH (Bexbach, Germany). The fabrication process is as follows.

1. The steel and the inner glass surfaces are cleaned to provide a dust and grease free surface. Unlike some adhesive interlayers, application of primer is not required prior to lamination to achieve good adhesion quality.
2. Subsequently, three layers of a 2 mm VHB (3M) clear acrylic tape is applied along three glass edges (shown in red in Fig. 3-1) to pre-bond the two glass plies. In this way, a 6 mm gap (clearance) is also formed between the two glass plies that provides a controlled envelope for resin injection (Fig. 3-1).
3. Hot-melt (HMA) is applied externally along the three VHB bonded edges of the glass assembly with the aid of a gun. These edges are further sealed with aluminium tape to eliminate potential leaks during resin injection (Fig. 3-2).
4. A jig was built to hold the steel insert in position and in correct alignment with the glass during assembly. The jig has a capacity of four specimens and has a tolerance of ±1 mm from the nominal geometry (Fig. 3-2).
5. The final step involves the resin injection within the glass assembly. The total volume of the resin required was calculated to compensate for the resin shrinkage (3 %) during the curing phase to ensure a complete filling of the finished specimens. Aluminium tape was used to form a suitable funnel along the entire length of the filling edge (glass embedment edge) (Fig. 3-2).

A visual inspection of the specimens at the end of the curing period revealed the formation of relative small (≃ 1 mm diameter) bubbles at the end face (Fig. 2-1) of the steel insert due to air trapped during the resin injection (Fig. 3-2).

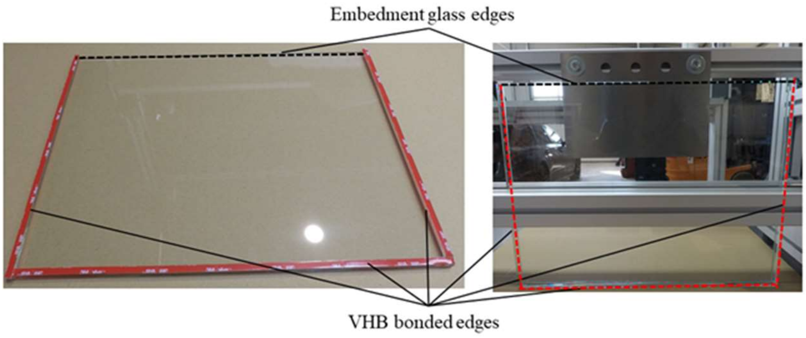

Figure 3-1 Glass ply with VHB tape (left) and glass assembly (right).

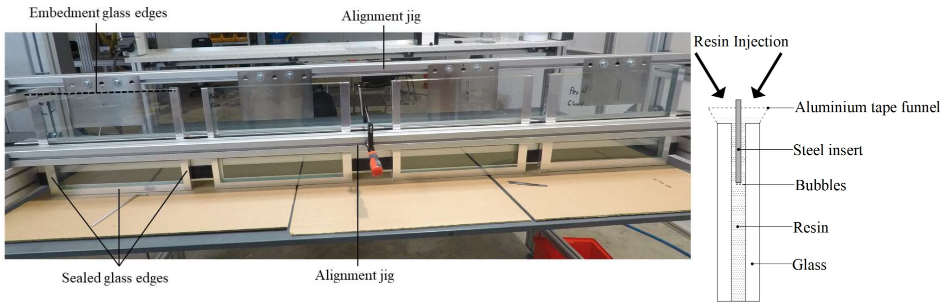

Figure 3-2 Photo of alignment jig (left) and scheme of resin injection (right).

4 Numerical Investigations

A 3D Finite Element model of the pull-out tests was constructed in Abaqus in order to identify the complex stress state and the principal failure mechanisms of the connection. The glass is modelled as linear elastic material (E_{glass}=70 GPa; υ_{glass}=0.23) and the steel insert as elasto-plastic material (E_{steel}=193 GPa; υ_{steel}=0.3) where the yield and ultimate stresses are 200 MPa and 500 MPa ($\varepsilon_{ultimate}$=40 %) respectively. The resin interlayer is modelled as linear viscoelastic material based on the generalised Maxwell model which in Abaqus is approximated with a Prony-series. Solid brick elements (C3D8R) are assigned to all materials. The mesh is refined at the embedded area (elements size of 1 mm) while a coarse mesh is defined at the end edges (maximum element size of 11 mm).

The load is firstly applied to the steel insert and then it is transferred to the glass plies via the resin interlayer. This is achieved by two distinct load-transfer mechanisms:

Load-transfer at the top-bottom and side faces (Fig. 2-1) of the steel insert which results in shear stresses in the interlayer. This mechanism generates shear stresses which are applied at the inner surface of the glass plies. The eccentricity of these stresses with respect to the centroid axes of the glass produces out-of-plane bending which results in normal tensile stresses located at the outer glass surface in the region of the end face of the insert (Fig. 4-1).

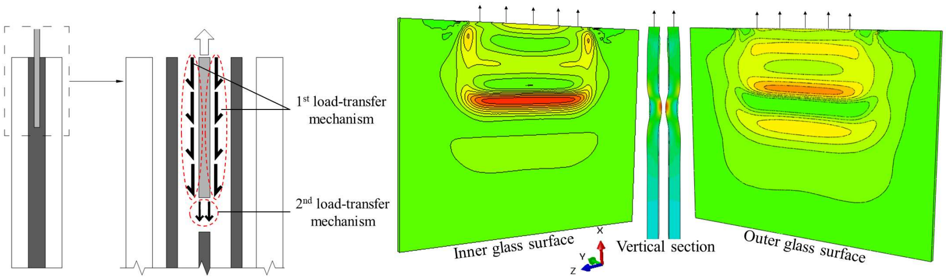

Figure 4-1 Load-transfer mechanisms (left), distribution of maximum principal tensile stresses and deformed shape of glass plies (right).

Load-transfer at the end face of the steel insert (Fig. 2-1) which results in normal tensile stresses at the interlayer. The resin is highly confined (ε_z =0) and almost incompressible (ε_x+ε_y+ε_z=0) due to its high Poisson's ratio ($\upsilon_{resin}\simeq 0.5$). Therefore, a small in-plane deformation produces an equal and opposite out-of-plane deformation (ε_y=-ε_x), which produces high normal tensile stresses at the inner surface of the glass plies in the vicinity of the end face of the steel insert (Fig. 4-1).

5 Tests setup

The first round of the full experimental program consists of five pull-out experiments all executed at Cambridge University Structures Laboratory using an Instron electro-mechanical testing machine, fitted with a 150 kN load cell. The tests are carried out at ambient laboratory temperature (22 °C ± 2 °C) and in displacement control with a crosshead displacement rate of 1 mm/min.

The specimens are placed vertically (Fig. 5-1) and the protruding part of the steel insert is pin-connected (5M12 of grade 8.8) to two (one at each side) steel clamping plates (1.4404, EN 10088-3:2005). These steel clamping plates are then fixed to the crosshead of the Instron machine with a pinned (M20 of grade 8.8) connection. The specimens are clamped to the machine by means of two symmetrically placed steel reaction bars (1.4404, EN 10088-3:2005) which are directly fixed to the Instron base via four steel threaded rods (grade 8.8, ISO 898-1:2009). The steel reaction bars are placed relatively close to the steel insert (15 mm clearance) to minimize load eccentricity. Pure aluminium sheets of thickness 6.35 mm are placed at the top glass edges to avoid direct contact between the glass and the steel reaction bars. The total applied load and the crosshead displacement are recorded. A laser extensometer is also used to measure the relative displacement between the steel insert and the glass.

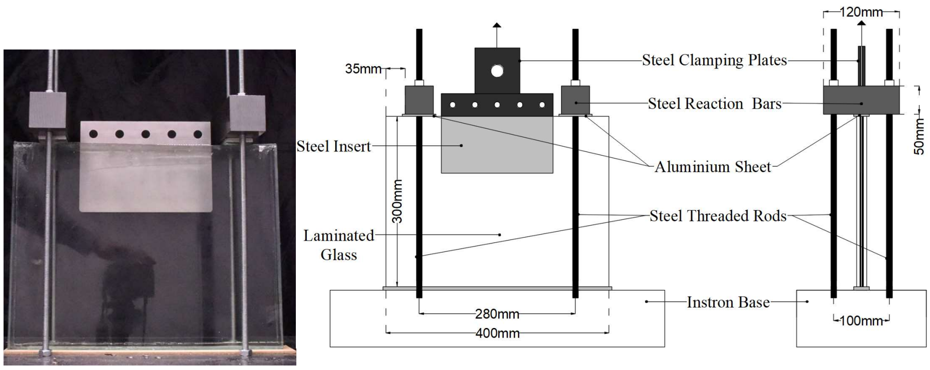

Figure 5-1 Scheme of the test setup; photo (left), frontal view (middle) and lateral view (right)

6 Experimental Results

Figure 6-1 shows the typical force-displacement curve of the pull-out tests. It is observed that the initial linear response up to approximately 40 kN, is followed by an elasto-plastic (softening) behaviour. This reduction in stiffness is attributed to yielding of the insert in the vicinity of the boltholes where high stress concentrations occur, in conjunction with progressive debonding of the insert along its end face where bubbles were observed during the fabrication process. As these stress concentrations increase with the applied load, the insert reaches its ultimate strength which corresponds to a maximum connection strength of about 87 kN. After this point, the load-displacement behaviour is almost perfectly plastic up to a maximum displacement of 9.9 mm at which point one of the glass plies fractures.

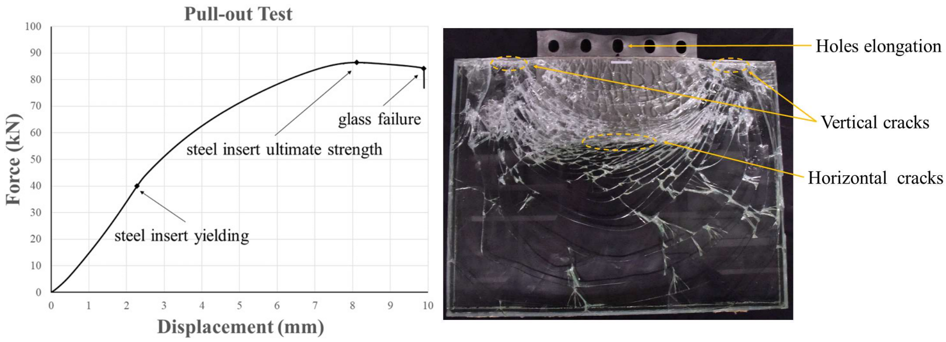

Figure 6-1 Typical force-displacement curve (left) and failure mechanism (right).

The failure mechanism of the connection is governed by failure of the steel insert which manifests in high elongation in the vicinity of the boltholes (Fig. 6-1). This results in significant ductility prior to failure of the glass and is deemed as a ‘safe’ failure mode. The glass breakage is observed at a load slightly lower than the connection pull-out strength due to the sub-critical crack growth phenomenon. The origin of glass failure appears to be in the vicinity of the steel reaction bars (vertical cracks). These cracks propagate in the glass surface across the location of the insert (horizontal cracks). The crack pattern matches the distribution of the maximum principal tensile stresses (Fig. 4-1) obtained from the FE analysis.

7 Summary and Conclusions

In this study, the fabrication methodology of an embedded liquid laminated glass connection is presented alongside the numerical and experimental results from pull-out tests conducted on physical prototypes of the connection.

The prototype specimens achieved a satisfactory aesthetic quality and confirmed that such specimens can be reliably and consistently manufactured. The pull-out tests showed a considerable connection strength of 87 kN. The principal connection failure mechanism is associated with failure of the steel insert which precedes the brittle glass breakage, thus providing considerable ductility. This failure mechanism is also confirmed by the 3D Finite Element analysis.

The excellent performance of the prototype connection merits further detailed investigation prior to implementation in real-world glass applications. In this regard, further pull-out tests will be conducted at different temperatures and strain rates to account for the time-temperature behaviour of the resin interlayer. These experimental data will be used to validate the numerical model of the connection so that it can be used as a predictive tool for sizing and optimising such connections, including the use of different insert materials.

8 Acknowledgements

The support of H. B. Fuller | Kömmerling and seele in providing the materials needed for this study is gratefully acknowledged .In addition, the authors would like to thank TTec GmbH and H.B. Fuller | Kömmerling for providing technical support for the specimens fabrication. This research project is part-funded by the EPSRC (UK) Doctoral Training Account.

9 References

[1] Overend, M.; Nhamoinesu, S.; Watson, J.: Structural Performance of Bolted Connections and Adhesively Bonded Joints in Glass Structures. In: Journal of Structural Engineering, Volume 139, Issue 12, 2013

[2] O'Callaghan, J.: An all glass cube in New York City. In: Glass Performance Days 2007, 2007, 98-101

[3] Torres, J.; Guitart; N.; Teixidor, C.: Glass fins with embedded titanium inserts for the façades of the new Medical School of Montpellier. In: Glass Structures and Engineering journal , Issue 2, 2017, pp 201-219

[4] Belis, J.; DE Visscher, K; Callewaert, D.; Van Impe, R.: Laminating metal-to-glass: preliminary results of case study. In: Glass Performance Days 2009, 2009, 191-193

[5] Puller, K.; Sobek, W.: Load-carrying behaviour of metal inserts embedded in laminated glass. In: Challenging Glass 3, 2012, 307-314

[6] Carvalho, P.; Cruz, P.J.S.; Veer, F.: Connecting Through Reinforcement – Experimental Analysis of A Glass Connection Using Perforated Steel Plates. In: Challenging Glass 3, 2012, 187-194

[7] Marinitsch, S.; Schranz, C.; Teich, M.: Folded plate structures made of glass laminates: a proposal for the structural assessment. In: Glass Structures and Engineering journal, Issue 1, 2016, pp 451-460

[8] Santarsiero, M.; Louter, C.; Nussbaumer, A.: Laminated connections for structural glass components: a full-scale experimental study. In: Glass Structures and Engineering journal, Issue 2, 2017, pp 79-101

[9] Santarsiero, M.; Bedon, C.; Louter, C.: Experimental and numerical analysis of thick embedded laminated glass connections. In: Composite Structures, 188, 2018, pp 242-256

[10] Bedon, C.; Santarsiero, M.: Laminated glass beams with thick embedded connections – Numerical analysis of full scale specimens during cracking regime. In Composite Structures, 195, 2018, pp 308-324

[11] Louter, C.; Santarsiero, M.: Metal-to-glass Bond Strength of Structural PVB. In: Glass Performance Days 2019, 2019, 49-55

[12] Wittwer, W.; Schwarz, T.: A material law for shear load and creep behaviour of glass laminates. In: COST Action TU0905 Mid-term Conference on Structural Glass, 2013, 377-388